

Cryptic Species in a Morphospecies Complex of Heterotrophic Flagellates: the Case Study of *Caecitellus* spp.

Klaus HAUSMANN¹, Petra SELCHOW¹, Frank SCHECKENBACH², Markus WEITERE² and Hartmut ARNDT²

¹Division of Protozoology, Institute of Biology / Zoology, Free University of Berlin, Berlin, Germany; ²Department of General Ecology and Limnology, Zoological Institute, University of Cologne, Cologne, Germany

Summary. Recent molecular studies have revealed quite different genotypes within morphospecies of heterotrophic nanoflagellates (HNF) as identified by light microscopy, e.g. for *Caecitellus parvulus*, known as one of the 20 most common heterotrophic flagellates worldwide. We combined molecular and morphological analyses to clarify if the morphospecies *Caecitellus parvulus* includes genetically as well as ultrastructurally and behaviourally distinguishable species with or without a different geographical distribution. Therefore we compared the ultrastructure, the small subunit of the ribosomal DNA (SSU rDNA), the growth rates as well as the locomotion patterns of two strains of *C. cf. parvulus* isolated from deep sea sediments and from the surface water of the oligotrophic Angola Basin, South Atlantic. The reconstruction of the kinetid architecture of two strains of *C. cf. parvulus* revealed differences in the number of microtubules in flagellar root 3, which surrounds the oral region and forms the cytoskeleton of the feeding basket. The number of microtubules in this region is also different from the description given earlier in the literature for *Caecitellus parvulus*. Additionally, there are significant differences between the two studied strains in the length of their posterior flagellum, their locomotion velocity and their moving pattern as well as in their growth rates. These observations, together with the results of the molecular comparison of the SSU rDNA of 11 different strains of *Caecitellus*, suggest the existence of at least three distinguishable species. Our results indicate cryptic speciation within the morphospecies *Caecitellus parvulus*. We describe two new *Caecitellus* species, i.e. *Caecitellus paraparvulus* and *Caecitellus pseudoparvulus*, which have been newly established within a *Caecitellus*-complex.

Keywords: *Caecitellus paraparvulus* n. sp., *C. pseudoparvulus* n. sp., cryptic species, heterotrophic flagellates, species complex.

INTRODUCTION

Heterotrophic flagellates are major consumers of bacteria, cyanobacteria and microalgae in a large variety of aquatic ecosystems. Consequently, they play an

important role as nutrient remineralizers and are mainly responsible for the carbon transfer to higher trophic levels in both pelagic and benthic environments of the oceans (e.g. Fenchel 1982a, Azam *et al.* 1983, Gasol and Vaqué 1993). In natural planktonic assemblages, the abundances of heterotrophic flagellates range from 10² to 10⁵ cells per ml (Berninger *et al.* 1991). Despite their high abundance and their importance in aquatic ecosystems, little is known about the biogeography and species-level diversity of many heterotrophic nanoflagellates (Preisig *et al.* 1991, Lee and Patterson 1998, Arndt *et al.*

Address for correspondence: Klaus Hausmann, Division of Protozoology, Institute of Biology / Zoology, Free University of Berlin, Königin-Luise-Str. 1-3, D-14195 Berlin, Germany; FAX (+49) 30 83 85 64 77; E-mail: hausmann@zedat.fu-berlin.de

2000). The question of the biodiversity and distribution of global free-living protists in general is still being intensively discussed (e.g. Foissner 1999, Finlay 2002). Some studies have been carried out to clarify the question of ubiquitous dispersal or endemism of protozoan species by investigating extreme habitats such as the deep sea or even hydrothermal vents (Atkins *et al.* 2000, Hausmann *et al.* 2002, Arndt *et al.* 2003, Scheckenbach *et al.* 2005). The deep sea is an extreme habitat (high pressure, absence of light, poor nutrients concentration, low temperature) which covers more than 60 % of the earth's surface. Despite the vastness of this biotope, knowledge on deep sea organisms, especially on protists, is still very limited (Finlay 2002, Turley 2002).

Numerous protists found in the deep sea sediments are also known from surface waters, but others which have been found in the deep sea have not been reported from shallow waters (Hausmann *et al.* 2002, Arndt *et al.* 2003). There are several known mechanisms which could account for genetic exchange between protist populations from different habitats; the high probability of dispersal of small organisms through e.g. global oceanic circulation, the formation of resting stages or the formation and sinking of marine snow (Finlay 2002, Turley 2002) are examples of such mechanisms. Small sinking aggregates are micro-environments for many heterotrophic flagellates within the water column (Caron 1991, Turley 2002, Kiørboe *et al.* 2004), e.g. for *Caecitellus parvulus*.

The different views of the biodiversity of protists are tightly connected with the differences in understanding of what a species is (Schlegel and Meisterfeld 2003). According to Mayden (1997), there are over twenty different species concepts.

The alpha taxonomy of heterotrophic flagellates is based mostly on a morphospecies concept (Patterson and Lee 2000). Because of the small size of flagellates, electron microscopy has to be used for morphological taxonomic characterisation and to prove restricted distribution (Foissner 1999), but it is still not used for most field studies and species descriptions.

The application of molecular criteria suggests that behind traditional morphospecies a much greater number of physiological or molecular species is hidden (Patterson and Lee 2000).

The heterotrophic nanoflagellate *Caecitellus parvulus* (Griessmann 1913) Patterson *et al.* (1993) is one of the 20 most common heterotrophic flagellates worldwide (Patterson and Lee 2000) and has always been regarded as a single species (Larsen and Patterson 1990, Ekeboom

et al. 1995/1996, Patterson and Simpson 1996, Atkins *et al.* 2000, Al-Qassab *et al.* 2002, Lee *et al.* 2003). The small, biflagellated gliding cells inhabit sediments and particle surfaces. Their anterior flagellum beats stiffly from side to side as cells glide with the posterior flagellum trailing behind. The species was first assigned to the genus *Bodo* as *B. parvulus* (Griessmann 1913), but Patterson *et al.* (1993) revealed ultrastructural features which are not compatible with a bodonid flagellate and placed it in the new genus *Caecitellus*, which they regarded as "a genus of uncertain affinities". O'Kelly and Nerad (1998) reconstructed the kinetid architecture of this species and found a high similarity to the Bicosoecida. The new term Hamatores (Al-Qassab *et al.* 2002) groups *Caecitellus* together with the pseudodendromonads. Both taxa lack three partite mastigonemes but share ultrastructural characteristics with the bicosoecids. Therefore they are related to the stramenopiles (Al-Qassab *et al.* 2002).

However, molecular studies from Scheckenbach *et al.* (2005) revealed quite different genotypes within morphospecies of heterotrophic nanoflagellates, so far identified by light microscopy as a single species. Therefore the studied strains of *Caecitellus parvulus* which were collected during an expedition with the German RV METEOR (cruise 48/1, DIVA I, year 2000) from deep sea sediments and surface water of the oligotrophic South Atlantic, Angola Basin, are designated as *C. cf. parvulus*.

The goal of the present study was to clarify whether the morphospecies *Caecitellus parvulus* includes genetically as well as morphologically and behaviourally distinguishable species and whether or not these species have different geographical distributions. Therefore we compared their morphology and ultrastructural architecture, their locomotion behaviour and growth characteristics as well as the genotype of two strains of *C. cf. parvulus*, i.e. an isolate from the deep sea with a strain from the surface water. This approach opens a new way to study biodiversity in protists.

MATERIAL AND METHODS

Sampling and cultivation of organisms

The *Caecitellus cf. parvulus* strains examined in this study were collected in July 2000 during the METEOR cruise 48/1 (DIVA I) in the oligotrophic South Atlantic and the Angola Abyssal Plain (the coordinates of the sampling locations are given in Table 1). Clonal

cultures were established and kept in culture as described in detail in Scheckenbach *et al.* (2005).

For the ultrastructural studies, the strains *Caecitellus cf. parvulus* DQ220712 (deep sea) and DQ220713 (surface water) were cultured at 19°C in artificial seawater (23 ‰ salinity). Sterilised wheat grains were added as a polysaccharide supply.

Pseudobodo tremulans strain DQ220718 was isolated by A.P. Mylnikov from brackish water of the Baltic Sea. The *Caecitellus* strain with the GenBANK accession number DQ230538 has been retrieved from the “American Type Culture Collection” (ATCC50091) and was the subject of a previous analysis by O’Kelly and Nerad (1998). All strains sequenced in this study and all sequences retrieved from GenBANK are referred to by their GenBANK accession numbers.

Light microscopy

Observations were made using an inverted microscope (ZEISS Axiovert 200, equipped with differential interference contrast optics). Micrographs were taken with an OLYMPUS OM-2N camera. For applied morphological nomenclature see Fig. 7.

Scanning electron microscopy

Cells were fixed for 15 min at room temperature on 0.1% Poly-L-Lysine coated cover slips with the Parducz fixative (Parducz 1967). Fixed cells were washed 5 × 5 min in artificial sea water (23 ‰ salinity) and dehydrated in a graded series of ethanol. Cells were dried in a BAL-TEC CPD 030 apparatus. After coating with gold in a BALZERS UNION SCD 040 sputter device, cells were examined with a FEI Quanta 200 ESEM.

Transmission electron microscopy

Cells were concentrated by centrifugation (200 rpm) and fixed for 30 min at room temperature in a fixative basically described by O’Kelly and Neard (1998).

After fixation the cells were transferred into agar blocks for better handling, dehydrated in a graded ethanol series, and embedded in araldit epoxy resin. Sections were made with a diamond knife, mounted on formvar-coated grids or slots and stained with uranyl acetate and lead citrate. They were examined with a PHILIPS EM 208 or a PHILIPS 120 BIO TWIN.

Table 1. Strain identifiers, sources of isolation and lengths of 18S rDNA of *Caecitellus cf. parvulus* strains sequenced in this study. Strain identifiers correspond to GenBANK accession numbers.

Accession number	Source	Sequence length
DQ220712	19°17.4’S 3°52.2’E, - 5424 m Angola Abyssal Plain, South Atlantic Ocean	1631
DQ220713	17°04.9’S 4°40.8’E, - 1 m South Atlantic Ocean	1646
DQ220714	19°17.4’S 3°52.2’E, - 5424 m Angola Abyssal Plain, South Atlantic Ocean	1669
DQ220715	19°19.8’S 3°55.6’E, - 5425 m Angola Abyssal Plain, South Atlantic Ocean	1681
DQ220716	16°23.1’S 5°27.0’E - 5388 m Angola Abyssal Plain, South Atlantic Ocean	1684
DQ220717	18°25.3’S 4°44.0’E, - 5392 m Angola Abyssal Plain, South Atlantic Ocean	1676
DQ230538	Sargasso Sea, - 100 m North Atlantic Ocean	1696

Table 2. P-distances of *Caecitellus parvulus* in percent (pairwise-deletion option set). Strain identifiers refer to GenBANK accession numbers. Strains sequenced in this study are in bold.

	(1)	(2)	(3)	(4)	(5)	(6)	(7)	(8)	(9)	(10)	(11)
AF174368 (1)											
AF174367 (2)	0.00										
DQ220715 (3)	4.55	4.44									
DQ220716 (4)	4.60	4.49	0.00								
DQ220713 (5)	4.39	4.39	0.00	0.00							
AY827847 (6)	4.54	4.55	0.00	0.00	0.00						
AY827848 (7)	4.65	4.66	0.12	0.12	0.13	0.12					
DQ220717 (8)	4.48	4.49	0.06	0.12	0.00	0.06	0.12				
DQ220714 (9)	4.38	4.39	0.00	0.00	0.00	0.00	0.12	0.00			
DQ220712 (10)	5.96	5.96	5.28	5.28	5.30	5.28	5.50	5.28	5.28		
DQ230538 (11)	5.85	5.86	5.55	5.60	5.24	5.54	5.46	5.20	5.17	0.00	

Locomotion analysis

Gliding cells of the *Caecitellus* strains DQ220712 and DQ220713, both grown at 19°C, were documented using an S-VHS video unit (JVC TK-1085E video camera, JVC TM-1500PS monitor, JVC BR-S600E video recorder). The velocity of gliding cells was measured by means of frame-by-frame analysis over the time cells needed to glide 10 µm straight forward. The movement of the anterior flagellum was studied in detail by measuring angles and times of the flagellar stroke. The angle was measured from the assumed median line of the cell (0°) to the outermost right (A) and left (B) point of the stroke (Fig. 1).

Growth experiments

The food provided for the *Caecitellus* strains DQ220712, DQ220713 and DQ230538 in these experiments was the heterotrophic bacterium *Halomonas halodurans*, grown in artificial seawater (23 ‰ salinity) with 0.1 % yeast extract added. Bacterial cultures were grown on a shaker at room temperature. After three days they were heat-killed to prevent overgrowth, harvested by centrifugation and resuspended three times in fresh artificial seawater.

All strains of *Caecitellus* were grown in sterile 50 ml tissue culture flasks (Sarsted, Newton, USA) with the addition of 10⁸ heat-killed bacteria ml⁻¹. This abundance is far above a threshold concentration for food limitation (Boenigk and Arndt 2002) and provides optimal growth conditions. In order to estimate the number of bacteria in the cultures, 50 µl subsamples were taken. The samples were fixed with 1% glutardialdehyde, stained with 0.1 mg ml⁻¹ DAPI (Porter and Feig 1980), retained on a black 0.2 µm polycarbonate filter and counted using a ZEISS Axioskop equipped with epifluorescence facilities.

The cultures were grown continuously at 19°C. Two independent replicates were considered for each of the three stains. The growth rates (r , d⁻¹) were calculated with the help of the abundances determined during the exponential growth phase: $r = \ln(N_1) - \ln(N_0)$. N_0 is the abundance at the start of the experiment and N_1 the abundance after one day. The doubling time (DT, h) was then calculated with the help of the growth rate: $DT = (\ln(2)/r) * 24$.

DNA extraction, SSU rDNA amplification and sequencing

DNA was extracted using a modified CTAB procedure (Clark 1992). The small subunit rDNA was amplified and sequenced as described in detail in Scheckenbach *et al.* (2005).

DNA sequence analysis

Determined sequence fragments were assembled manually and unambiguously aligned together with other sequences retrieved from GenBank using the ClustalX multiple alignment program version 1.83 (Thompson *et al.* 1994). Uncorrected genetic distances (p -distances) were calculated using MEGA version 3.0 (Kumar *et al.* 2004) with pairwise-deletion option set. Phylogenetic analyses were performed by using the maximum likelihood (ML) (Felsenstein 1981), maximum parsimony (MP) (Swofford and Olsen 1990) and minimum evolution (ME) (Rzhetsky and Nei 1992) methods. The precision of the internal nodes was assessed by bootstrapping (Felsenstein 1985). For ML analysis the transition/transversion ratio was set to 1.24. The model of nucleotide substitution used for ME analysis was LogDet (Lockhart *et al.* 1994, Steel 1994). For ML and MP analysis,

PHYLIP version 3.63 was used (Felsenstein 2004); MEGA version 3.0 was used for ME analysis.

RESULTS

Overall structure

Caecitellus cf. parvulus from the deep sea (DQ220712) and from the surface water (DQ220713) is a biflagellate cell with a slightly rounded triangular profile. The body shape appears angular because of a large feeding basket protruding on the ventral-apical side (Figs 2, 3). The basket is internally supported by a horseshoe-shaped cytoskeletal structure of numerous microtubules; these microtubules are also mainly responsible for the characteristic form of the mouth region. The large ingestion apparatus is easily observable even under a light microscope (Figs 2, 3). SEM micrographs clearly show that a lip surrounds the rim of the oral apparatus (Figs 4-6). The cell length varies from 2.0 to 4.5 µm. Two flagella of unequal length originate from the apical-ventral side of the cell (Figs 2-6). The anterior flagellum projects forward and beats laterally in a stiff manner. It is about 1.5 × the length of the cell body in both strains of *Caecitellus* (Figs 4-6). The cell usually glides smoothly

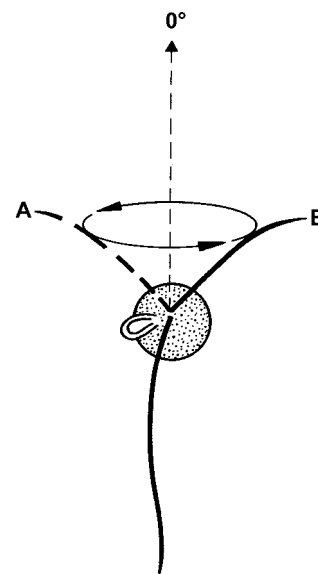
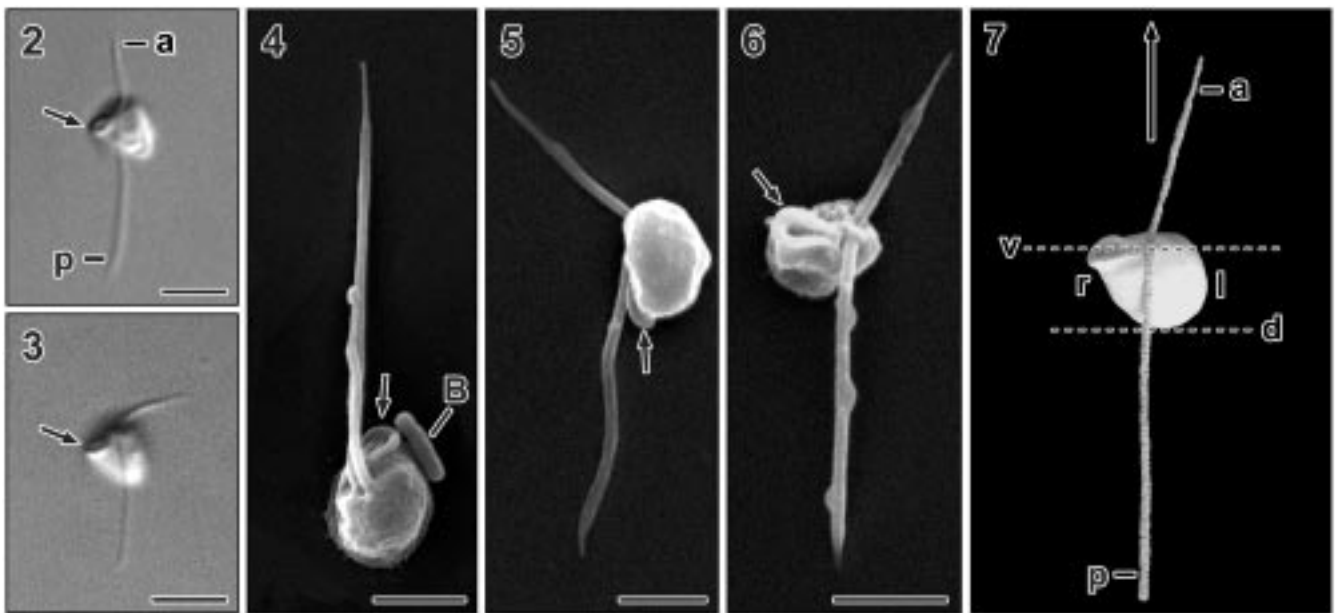


Fig. 1. Scheme depicting the rotating movement of the anterior flagellum. The time needed for a complete flagellar stroke was measured as well as the maximum angles of deflexion to the outermost left (A) and right point (B) from an assumed median line of the cell (0°).



Figs 2-6. Light and scanning electron micrographs of *Caecitellus*. **2, 3** - differential interference contrast light micrographs, ventral view of living cells (**2** - deep sea strain DQ220712; **3** - surface water strain DQ220713), arrow - ingestion apparatus; **4-6** - scanning electron micrographs showing a lip surrounding the rim of the oral apparatus (arrow); **4** - cell of strain DQ220712 with adjacent bacterium (B); **5, 6** - lateral views of strain DQ220713 cells; **7** - clay model of *Caecitellus* illustrating the in this study applied nomenclature: a - anterior flagellum, p - posterior flagellum, d - dorsal, v - ventral, l - left, r - right, arrow - direction of locomotion. Scale bars: 5 μ m (**2, 3**); 2 μ m (**4-6**).

forward along its fully extended posterior flagellum, which trails underneath the cell body and shows significant differences in length between the two strains DQ220712 and DQ220713 (Fig. 8).

TEM micrographs (Figs 9-12) show that cells from both *Caecitellus* strains generally follow a similar basic structural plan. For example, three microtubular roots originate from the two basal bodies: one compactly structured root (R3) and two less complex roots (R1 and R4) (Figs 9, 10) (nomenclature according to O'Kelly and Nerad 1998).

The cells are uninucleate and contain mitochondria with tubular cristae. One mitochondrion is always located close to the nucleus at its ventral side and is associated with the compact root (R3) at the right side of the cell, next to so-called electron lucent bodies (Fig. 11). There is only one dictyosome per cell, which is located close to the nucleus and dorsal to the flagellar basal bodies (Fig. 12).

The glycocalyx of the DQ220712 strain appears as a relatively thick electron dense layer (Figs 9, 11) compared to the glycocalyx of the DQ220713 strain which is hardly recognisable at all (Figs 10, 12). The thick glycocalyx layer covers the complete cell surface includ-

ing flagellar pocket, cytostome as well as the two flagella.

The flagellar apparatus

The kinetid contains two basal bodies (1 and 2), one broad and complex microtubular root (R3) and two simple ones (R1 and R4) (Figs 9, 10), a striated band (Figs 16-18) and a connecting fibre (Fig. 19).

The two basal bodies are linked together by a connecting fibre and to R3 by a striated band. The latter leads from the right hand side of basal body 2 as far away as the point of separation of R3 (Figs 18, 19). It runs slightly anterior to R3 (Fig. 14) and has a connection to basal body 1. The connecting fibre extends between the bases of the two basal bodies from the left hand side of basal body 2 towards the base of basal body 1 (Fig. 19).

The basal bodies of the posterior (1) and anterior flagellum (2) are each approximately 0.5 μ m long and oriented to each other in an L-shaped manner. Their longitudinal axes do not run coplanar, but are shifted approx. 0.15 μ m to each other and are slightly laterally tilted. Electron-dense material is located in the proximal lumen of the basal bodies (Fig. 12, arrow). Cross

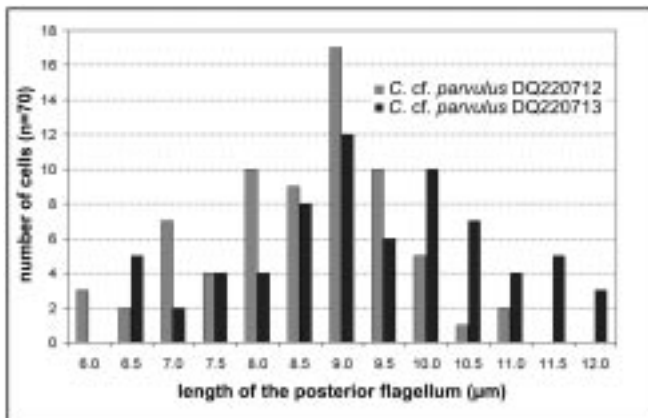


Fig. 8. Diagram showing significant ($p < 0.001$; $z = -3.311$; U-test) differences in the length of the posterior flagellum of *Caecitellus* cf. *parvulus* strain DQ220712 (deep sea) and strain DQ220713 (surface water).

sections of this region clearly show the kinetosomal $9 \times 3 + 0$ structure (Fig. 13). There is a basal axonemal plate at the level of the plasmalemma (Fig. 12, arrow-head).

R1, composed of two microtubules, originates in an electron-dense material on the right side of basal body 2 (Figs 9, 19) at its midregion and extends to the dorsal surface to the left side of the cell (Fig. 12). R3 consists of three subunits: the abc subunit, the 8-35 subunit [(in strain DQ220713; named 8-29 subunit in strain DQ220712) and the x subunit (Figs 9, 10)].

At the origin of R3, which lies at the ventral side of the proximal end of basal body 2, the root consists initially of eight microtubules (Fig. 13). After a short distance three more microtubules are added, which appear in cross section as an L-shaped structure with a typical $8 + 3$ pattern (Fig. 14). The three added microtubules are the abc subunit of R3. The subunit separates from the root (Figs 15, 16) and turns slightly to the left, forming a tight loop around the posterior flagellar insertion (Figs 19, 22).

The broadest subunit of R3, initially consisting of eight microtubules, increases in number up to 35 (Fig. 28) and passes to the right side of the ventral region, forming a loop that supports the peristome (Fig. 20). It then passes left and back to make contact with the abc subunit (Figs 9, 19). At the point of separation, R3 is associated with electron-dense material subtending the eight-microtubule subunit (Fig. 22). In the ascending root (Figs 11, 32), which is the broader subunit of R3, the number of

microtubules increases. In the deep sea strain (DQ220712) 35 microtubules (Fig. 28) and in the surface strain (DQ220713) as many as 29 microtubules (Fig. 29) have been detected. The highest number of microtubules is reached just before the turning point of the loop (Fig. 32). Figures 23-27 are serial sections through an oral apparatus. The section plane of these micrographs is indicated in Fig. 11 by a dotted line. The microtubules of the ascending side of the loop increase in number compared to the descending side of the loop (Figs 23-27).

These extra microtubules have no obvious connection to the basal bodies, whereas the junction of the large loop and the abc loop are visible in Figs 18, 19. Most microtubules of the descending root terminate before the two parts of the loop join. In Fig. 23 there are only five microtubules left in the descending root.

An individual microtubule called x runs parallel to the large loop (Figs 12, 20, 23-31). This microtubule has its origin close to the separation of R3 and extends to the outside of the loop in the lip at approximately the same level as the second microtubule from the 8-35 loop. In the area of the turning point of the x-microtubule, one additional microtubule is detectable directly underneath it (Figs 30, 31).

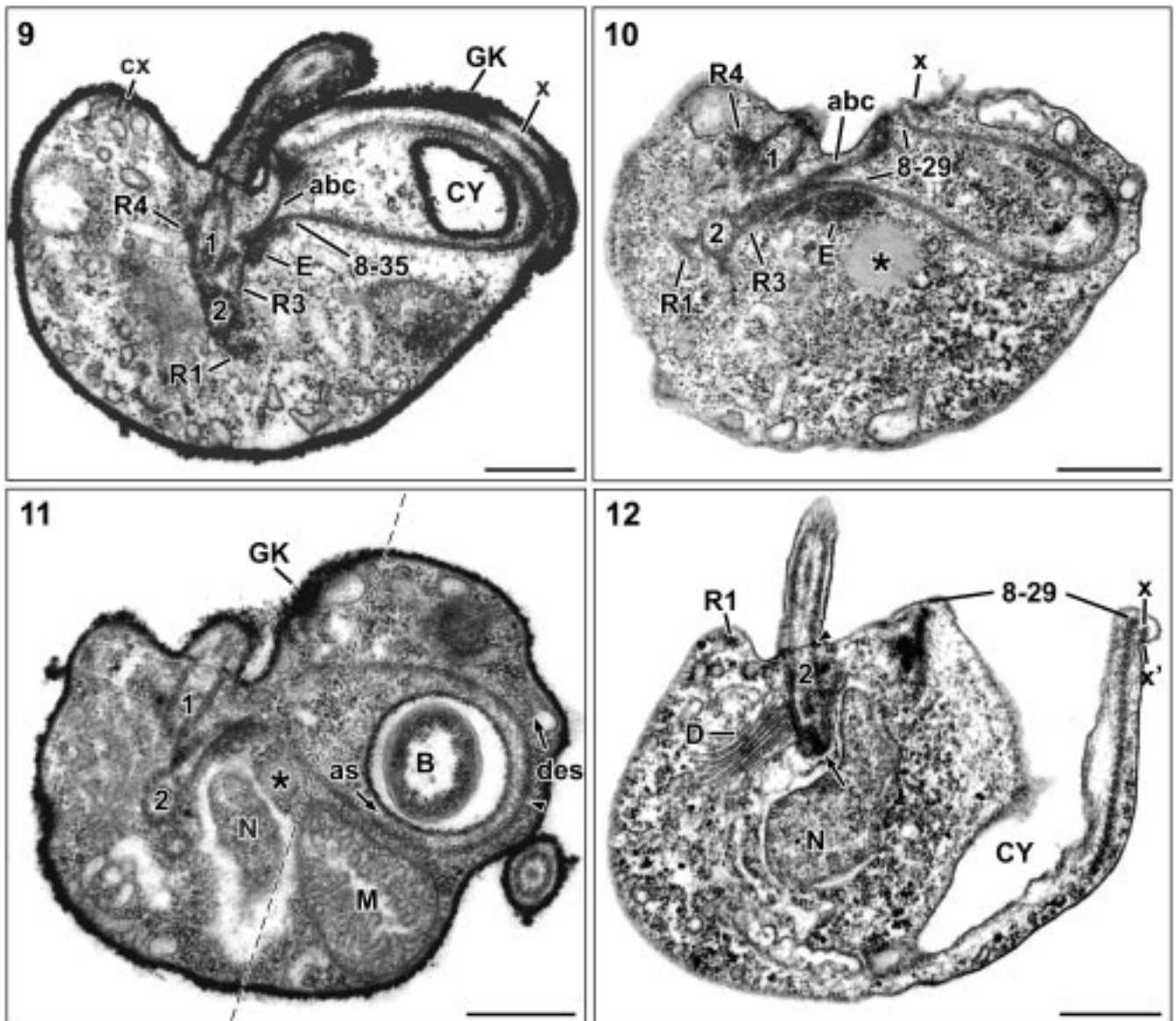
The end of R3 is made of the microtubules c and x (Fig. 32), which combine the small and the large loops at the left side of the cell and run around the insertion region of the posterior flagellum towards the dorsal apical cell side (Figs 18, 20).

R4 consists of only two microtubules which arise from the basal body of the anterior flagellum (Figs 9, 18, 22). It leads from the dorsally oriented part of the correspondent basal body to the left ventral side of the cell and terminates near the end part of R3.

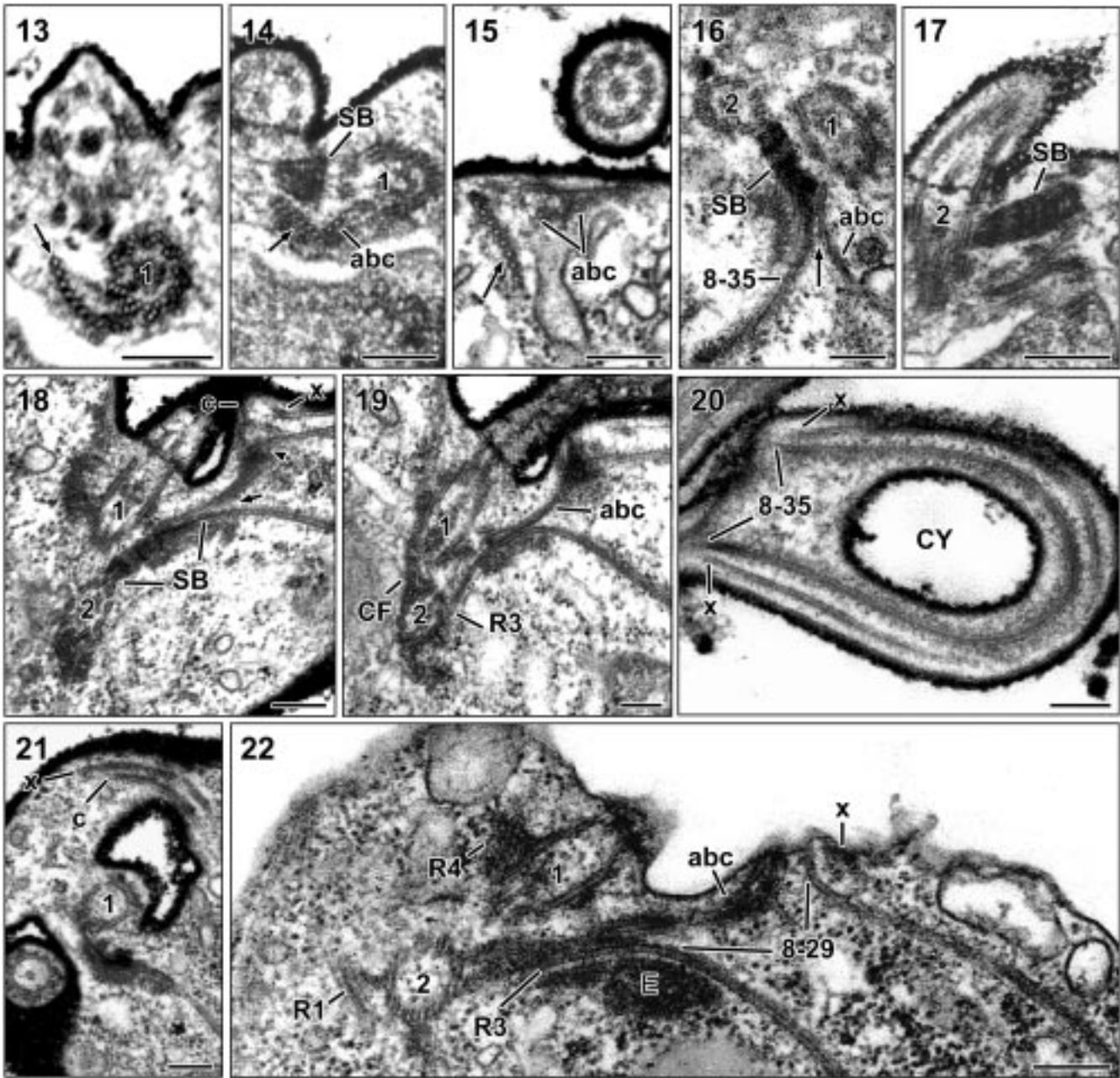
Summarizing the structural and ultrastructural features, the strains DQ220712 and DQ220713 show significant differences in the length of the posterior flagellum, the appearance of the glycocalyx and the maximal number of microtubules in R3.

Locomotion pattern

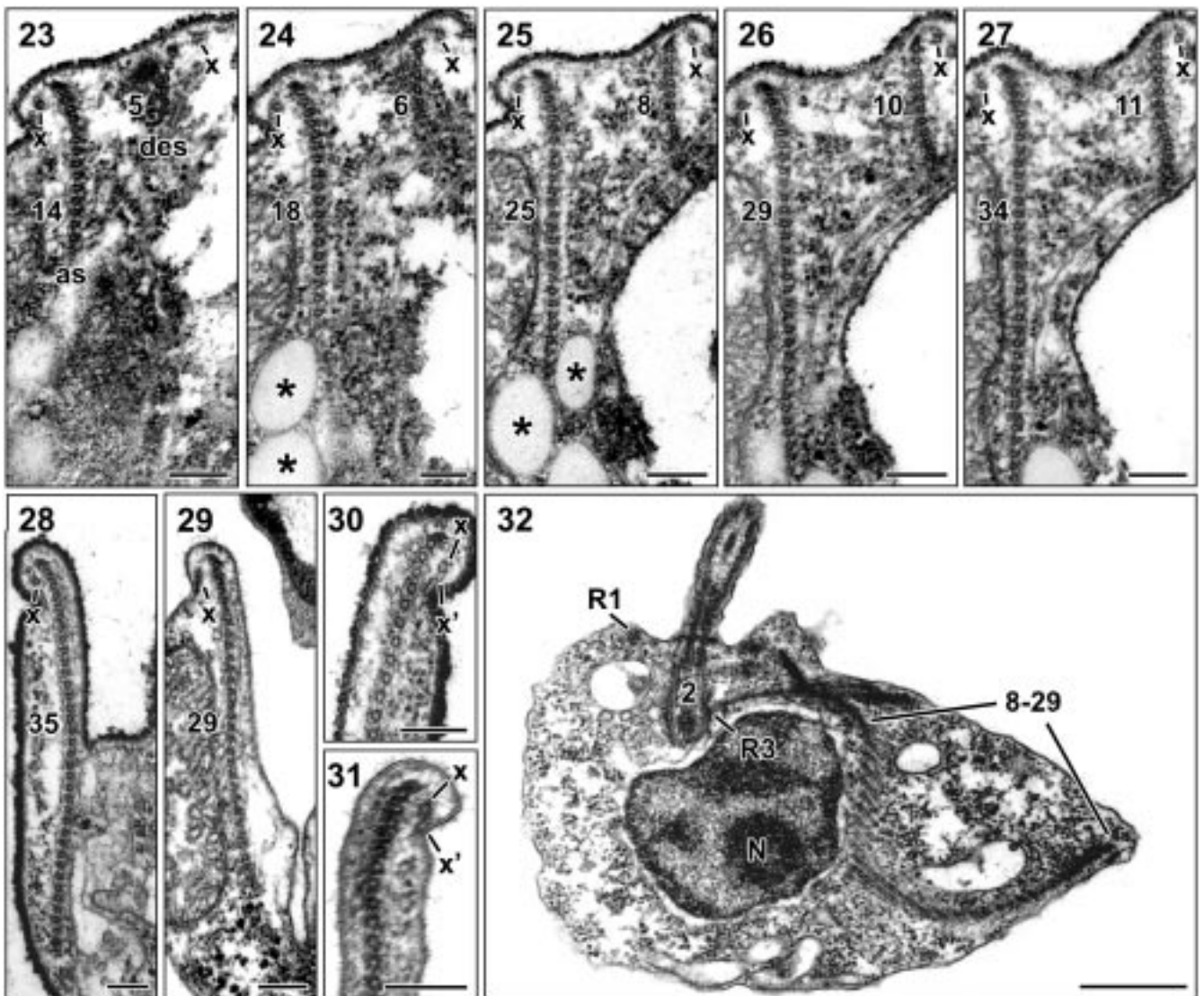
Both studied *Caecitellus* strains have a moving anterior and a trailing posterior flagellum; their locomotion patterns look therefore very similar. Nevertheless, Fig. 33 shows that significant differences in the velocity of the gliding cells were measurable (Fig. 33a), as well as in the angle the anterior flagellum describes when it moves (Fig. 33b) and in the time it needs for one circle (Fig. 33c). Cells of the surface water strain (DQ220713)



Figs 9-12. Transmission electron micrographs showing the general cellular organisation of the two examined *Caecitellus* strains [DQ220712, deep sea (**9**, **11**) and DQ220713, surface water (**10**, **12**)]; **9**, **10** - horizontal sections, viewed from anterior/dorsal showing microtubular root 1 (R1) and root 3 (R3) originating from basal body of anterior flagellum (2); R3 splitting into a short loop (abc), a large loop (8-35, resp. 8-29) and a single microtubule (x); electron-dense material (E) at separation point of abc loop and 8-35 loop, x-microtubule leading at the right side of the cell around the cytotome (CY); microtubular root 4 (R4) originating at basal body of posterior flagellum (1); **9** - microtubules c and x at the anterior/left side of the cell; GK - glycocalyx. **10** - electron-lucent body (asterisk) in close vicinity to ascending part of 8-29-loop; **11** - mitochondrion (M) with tubular cristae close to the nucleus (N) ventrally next to ascending part (as) of large loop of R3 and to the electron lucent bodies (asterisk); after turning point (arrowhead) large loop turning left, its descending part (des) passing along ventral side of the cell; bacterium (B) inside oral apparatus; dotted line indicates approximate section plane of Figs 23-27; **12** - longitudinal section of basal body 2 with electron-dense material in its proximal end (arrow) and with basal plate at level of the plasmalemma (arrowhead); dictyosom (D) close to the left of basal body 2 and the nucleus (N); prominent cytopharynx (CP) surrounded by basket of 8-29 microtubules; in the lip microtubule x' underneath microtubule x; root 1 (R1) directly underneath the anterior surface at the left side of the cell. Scale bars: 0.5 μ m.



Figs 13-22. Kinetid architecture of *Caecitellus* (**13-21**: strain DQ220712, deep sea; **22**: strain DQ220713, surface water). **13** - cross section of the proximal end of basal body 1 (1) and R3 (arrow); **14** - cross section of L-shaped part of R3, basal body 1 and striated band (SB) at a point slightly distal to that of Fig. 10; R3 depicted as L-shaped structure with typical 8, 3 pattern, showing the start of separation of abc and 8 subunit of R3 (arrow); **15** - cross section of 8 subunit (arrow) and abc microtubules at a level distal to R3-separation; **16** - cross section of basal body 2 and oblique section of basal body 1, showing position of striated band (SB) and separation of R3 in abc subunit and 8-35 loop (arrow); **17** - oblique section of basal body 2 illustrating its association with striated band (arrow); **18, 19** - consecutive sections of the connecting structures of basal bodies 1 and 2: i) striated band (SB) and connecting fibre (CF), ii) proximal end of R3 with its point of separation (arrow) as well as junction of the descending 8-35 loop, iii) abc loop (arrowhead), iv) continuation of microtubules c and x at left side of the cell; **20** - longitudinal section of microtubule x and 8-35 loop leading around the cytostome (CY); **21** - distal end of R3 consisting of microtubules c and x leading around the insertion of the posterior flagellum (1). **22** - kinetid of *Caecitellus* cell strain DQ220713 (surface water), section through the dorsal anterior side of the cell showing i) basal bodies 1 and 2, ii) the origin of microtubular roots R1, R3 and R4, iii) parts of the subunits of R3 (8-29, abc, x). Scale bars: 0.2 μ m.



Figs 23-32. Microtubular structure of the feeding basket of *Caecitellus*. **23-27** - serial sections of a feeding basket of a cell of strain DQ220712 (section plane - dotted line in Fig. 11) showing i) increasing number of microtubules in ascending (as) and descending (des) part of 8-35 subunit of R3, ii) location of electron lucent bodies (asterisks), iii) position of microtubule x; **28** - ascending root with max. 35 microtubules (strain DQ220712) and in **29** with max. 29 microtubules in strain DQ220713; **30** - cell of strain DQ220712; **31** - cell of strain DQ220713 showing microtubule x' in the lip immediately underneath microtubule x in the area of the turning point of the loop; **32** - cell of strain DQ220713 in dorsal view illustrating basket structure of 8-29 loop (ascending subunit), origin of root 3 (R3) at basal body 2 anteriorly to the nucleus (N) and location of R1 at the left anterior side of the cell. Scale bars: 0.2 μm (23-27, 30, 31); 0.5 μm (28, 29, 32).

move faster forward and have an anterior flagellum which describes a smaller angle in less time than most cells of the studied deep sea strain (DQ220712).

Growth rates

The growth rates of the surface water strain (DQ220713) and deep sea strain (DQ220712) differed

distinctly with mean (\pm range) maximal growth rates of $3.13 \pm 0.48 \text{ d}^{-1}$ for the surface water isolate and $4.47 \pm 0.25 \text{ d}^{-1}$ for the deep sea isolate (Fig. 34). These growth rates mean doubling times of 5.4 and 3.7 h, respectively. With a mean (\pm range) maximal growth rate for the ATCC50091 strain of $5.34 \pm 0.04 \text{ d}^{-1}$ (mean doubling time: 3.1 h), this strain was more similar to the deep sea strain than to the surface water strain.

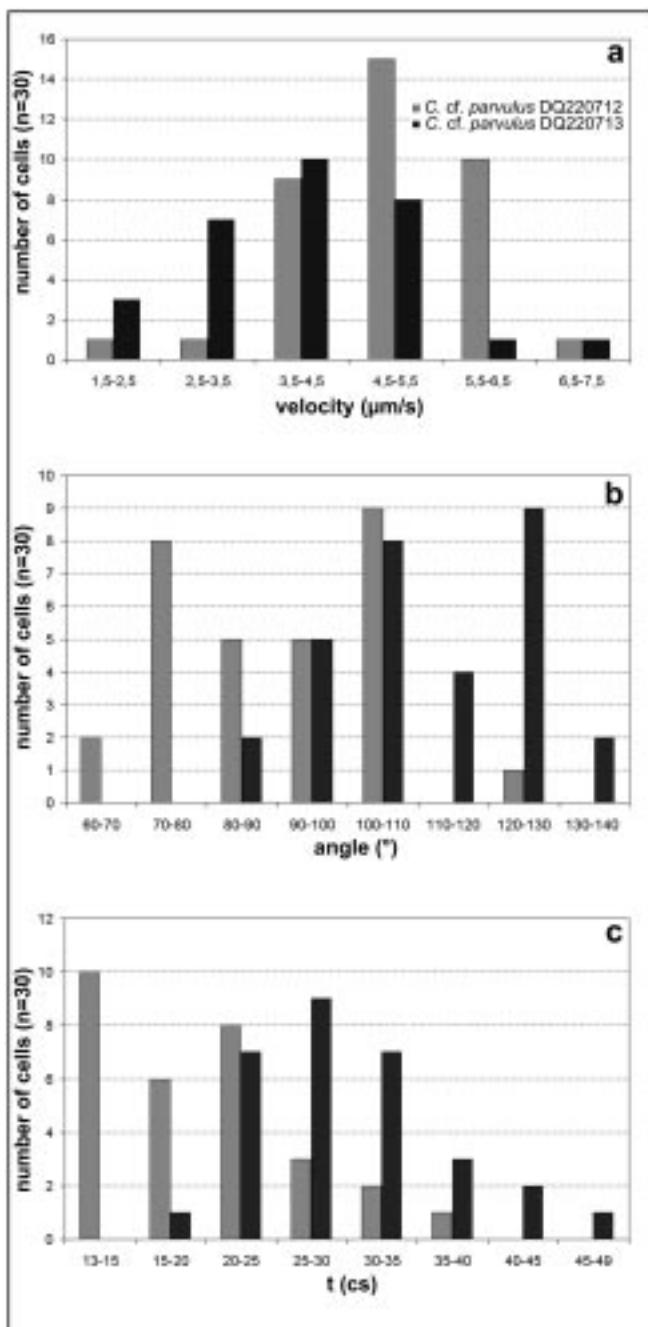


Fig. 33. The locomotion velocity of the two studied *Caecitellus* strains differs significantly (a) as well as the angle which the anterior flagellum describes during its activity (b). Also the time which is needed to complete one cycle of the anterior flagellum differs significantly (c).

Molecular data

All sequences of *Caecitellus parvulus* obtained in this study have nearly the same length as those reported

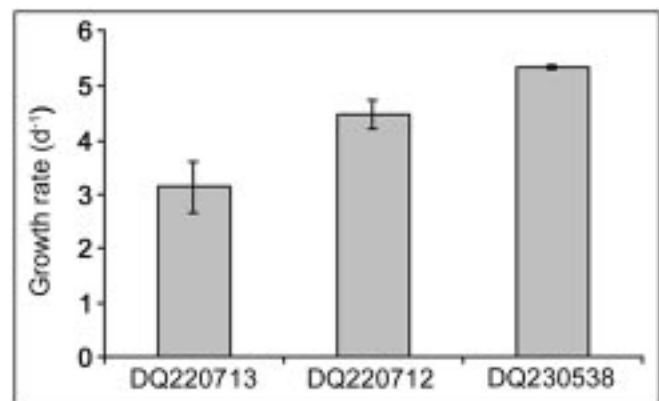


Fig. 34. Mean (\pm range) maximal growth rates of the *Caecitellus* strains DQ220713 (from the surface water of the South Atlantic), DQ220712 (from the deep sea of the South Atlantic) and DQ230538 (ATCC).

from previous studies (Table 1). After an initial phylogenetic analysis comprising a broad range of heterokont taxa, the labyrinthulid *Ulkenia profunda* has been chosen to root the tree. This initial analysis supported the placement of *Pseudobodo tremulans* as basal bicosoecid taxon (Karpov *et al.* 2001), although its placement at the root of the bicosoecids varies depending on the taxa and the numbers of sequences included in phylogenetic analysis. An unstable branching pattern has been observed regarding the bicosoecid *Symbiomonas scintillans*. This taxon has therefore been excluded from phylogenetic analysis. With the exception of *Cafeteria*, all phylogenetic methods recovered the same optimal tree topology, with each node supported by high bootstrap values (Fig. 35). In ML and MP analysis, *Cafeteria* branches at the root of the *Caecitellus* clade with moderate bootstrap support (ML: 65; MP: 52), in ME analysis at the root of the *Adriamonas/Siluania* clade (bootstrap value: 64).

The clade composed of both *Pseudobodo* strains (DQ220718: isolated by A.P. Mylnikov from brackish water of the Baltic Sea near Hiddensee, Germany; AF315604: isolated by A. P. Mylnikov from brackish water of the White Sea) branches first, followed by the clade composed of *Siluania*, *Adriamonas* and *Cafeteria* and finally the clade comprising the different strains of *Caecitellus*. The tree shows a paraphyletic family Siluaniidae (*Siluania*, *Adriamonas* and *Caecitellus*; Karpov *et al.* 2001) and Cafeteriidae (*Cafeteria* and *Pseudobodo*; Moestrup 1995), but discrepancies between morphological and molecular data concerning this

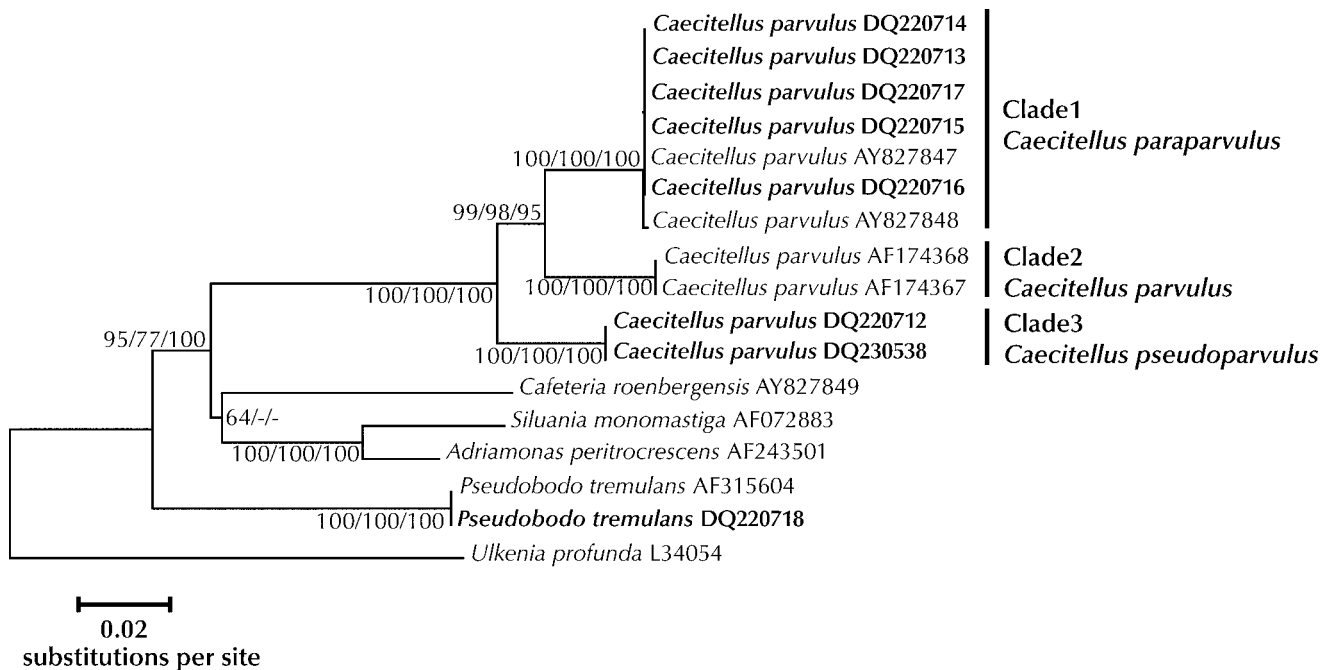


Fig. 35. Rooted minimum evolution bootstrap consensus tree of the order Bicosoecida (Grassé, Karpov 1998, using 1533 positions (nucleotide substitution model: LogDet; complete-deletion option set). The tree was rooted using *Ulkenia profunda* as outgroup. Numbers at the nodes are bootstrap support percentages from 250 replicates using the minimum evolution method (left) and from 100 replicates for both the maximum likelihood (middle) and maximum parsimony (right) methods. Strain identifiers refer to the GenBANK accession numbers. Strains sequenced in this study are in bold.

families are well known and have already been addressed in detail by Karpov *et al.* (2001).

In all trees obtained, *Caecitellus* forms a monophyletic group with three distinct clades and with very high bootstrap support values. The first clade (Clade 1) is composed of strains which were all isolated in 2000 from sediments of the Angola Abyssal Plain, with the exception of one strain (DQ220713), the ultrastructure of which is also subject of this study, taken from the surface water of the South Atlantic Ocean. The second clade (Clade 2) is composed of both strains sequenced by Atkins *et al.* (2000) isolated in 1995 from mussel beds of deep sea hydrothermal vents of the Eastern Pacific Rise (AF174367), respectively in 1996 from New Bedford Harbor, Massachusetts (AF174368). The third clade (Clade 3) is composed of the strain DQ230538 isolated in 1981 by P. G. Davis, the ultrastructure of which has been studied by O'Kelly and Nerad (1998) and of the strain DQ220712 isolated in 2000 from deep sea sediments of the Angola Abyssal Plain, the ultrastructure of which is subject to this study.

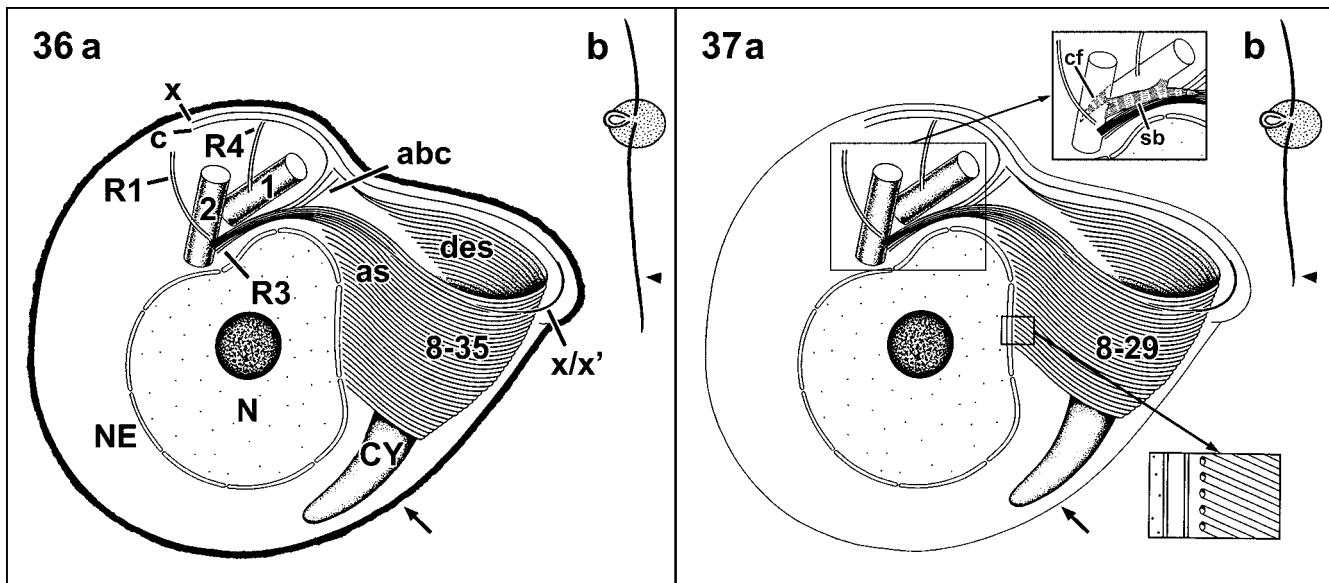
Uncorrected distances (*p*-distances) have been calculated for all strains of *Caecitellus* (Table 2) and show

very high ribosomal sequence divergences within this group, as well as for both *Pseudobodo* strains (0.20 %). Mean *p*-distances and their standard deviations have been calculated between the three major clades of *Caecitellus* as well as within these clades. Mean distances within all three clades are equally low with minimal variances (Clade1: 0.05 ± 0.03 %; Clade2: 0.00 %; Clade3: 0.00 %). On the other hand, very high mean distances with at the same time low variances can be observed in all three cases between these clades (Clade1/Clade2: 4.50 ± 0.50 %; Clade1/Clade3: 5.35 ± 0.52 %; Clade2/Clade3: 5.91 ± 0.54 %).

DISCUSSION

Morphological Data

At the level of light-microscopy there are no obvious structural differences visible between the two investigated *Caecitellus cf. parvulus* strains DQ220712 (from the deep sea) and DQ220713 (from the surface water). Their cell shape and way of movement seems to be in



Figs 36, 37. Schematic reconstruction of the position of the basal bodies 1 and 2, the paths of the flagellar roots R1, R3 and R4 in relation to the contour of the cell, the nucleus (N) and the cytopharynx (CY) in *Caecitellus cf. parvulus*, strain DQ220712 (**36a**) and strain DQ220713 (**37a**), dorsal view; feeding basket built of 8-35 (**36a**) or 8-29 (**37b**) microtubules with ascending (as) and descending (des) parts: separation of R3 into subunits abc, 8 and x; turning point with additional microtubule x' directly underneath x; microtubules c and x representing end of R3 at left/ventral side of the cell;; differences in the appearance of the glycocalyx of both strains are indicated by an arrow; **36b** and **37b** contour of a complete cell of *C. cf. parvulus*, strain DQ220712 (**36b**) and strain DQ220713 (**37b**) seen ventrally; arrowhead pointing to the differences in length of the posterior flagellum. Insets in **37** (the depicted features are identical in the two investigated strains): above: path of connecting fiber (cf) and striated band (sb); below: microtubules of feeding basket without intimate contact with nuclear envelop (NE).

conformity with almost all previous light-microscopical descriptions (e.g. Patterson *et al.* 1993, Tong 1997a, O'Kelly and Nerad 1998, Lee and Patterson 2000, Al-Qassab *et al.* 2002, Lee *et al.* 2003). An additional thread trailing from the outer margin of the mouth, noted only by Tong (1997b) and Tong *et al.* (1998), was not seen in the present study.

However, biometric analysis showed significant differences in the length of the posterior flagellum of the two studied strains of *C. cf. parvulus*. But the average length of the posterior flagellum in both strains is within the size range reported in the literature for *C. parvulus* (e.g. O'Kelly and Nerad 1998, Atkins *et al.* 2000, Al-Qassab *et al.* 2002, Lee *et al.* 2003).

The ultrastructural comparison of *Caecitellus cf. parvulus* strains DQ220712 and DQ220713 shows that in general both strains follow a similar basic structural plan, but there are differences in the appearance of the glycocalyx and in the maximal number of microtubules in the flagellar root 3 (R3).

Only in strain DQ220712 is the glycocalyx visible as a relatively thick, electron-dense layer. It is hardly

recognisable at all in strain DQ220713 and in all published TEM micrographs of *Caecitellus parvulus* (Patterson *et al.* 1993, O'Kelly and Nerad 1998). Differences in the morphological appearance of the glycocalyx are useful tools to differentiate e.g. between the amoeba genera *Vanella* and *Platyamoeba* at the ultrastructural level (Page and Blakey 1979). On the other hand, molecular studies have revealed that glycocalyx appearance is not necessarily also a reliable phylogenetic marker to distinguish between the genera in this case (Sims *et al.* 2002).

The kinetids of both ultrastructurally investigated *C. cf. parvulus* strains also differ from the kinetid of the described *Caecitellus parvulus* in the maximal number of microtubules found in R3, which forms the cytoskeletal fundament of the feeding basket. O'Kelly and Nerad (1998) counted a maximum of approximately 24 microtubules for *C. parvulus* (strain DQ230538 from the Pacific Ocean). With eleven microtubules more, strain *C. cf. parvulus* DQ220712 (from the South Atlantic deep sea) has a much larger feeding basket. Nevertheless, the feeding basket of *C. cf. parvulus* strain

Table 3. Summary of differences between the species of the *Caecitellus* complex.

Criteria	<i>Caecitellus</i> complex				
	<i>C. parvulus</i> Patterson <i>et al.</i> 1993	<i>C. pseudoparvulus</i> O'Kelly and Nerad 1998	<i>C. pseudoparvulus</i> Atkins <i>et al.</i> 2000	<i>C. paraparvulus</i> this study	<i>C. paraparvulus</i> this study
cell length	4-7 µm	3-7 µm	3-10 µm	2-4 µm	2.5-4.5 µm
ratio: anterior flagellum/cell length	?	1.5-2.5	1	1-2	1-2
ratio: posterior flagellum/cell length	?	2.5-3.5	3-4	2.5-4.5	2-4.5
glycocalyx	thin	thin	?	thick	thin
R1	?	2 mt	?	2 mt	2 mt
R3 (proximal)	?	8+3	?	8+3	8+3
R3 (maximal)	?	24 mt	?	35 mt	29 mt
x -mt (R3)	?	+	?	+	+
x' -mt (R3)	?	-	?	+	+
R4	?	2 mt	?	2 mt	2 mt
genetical distance to <i>C. parvulus</i>	?	?	?	5.91%	4.5%
genetical distance to <i>C. pseudoparvulus</i>	?	?	5.91%	?	5.35%
genetical distance to <i>C. paraparvulus</i>	?	?	4.5%	5.35%	?

? - not reported; R1, R3, R4 - root 1, 3, 4; mt - microtubule

DQ220713 (from the South Atlantic surface water) with its 29 microtubules is smaller than that of strain DQ220712, but includes still more microtubules than described for *C. parvulus* (O'Kelly and Nerad 1998).

The differences of the glycocalyx and the feeding basket could be indicative for a different ecological niche and/or geographic distribution, but the molecular data show that the three resulting morphological and genetically distinctive clades include strains from different habitats and locations. Whether or not the differences in the feeding basket size are coupled with differences in the size of their food (bacteria) is thus far unknown, but not unlikely.

Locomotion pattern

The difference between the gliding velocities of the two studied strains is significant, as are the dynamics of their anterior flagellum. This might attest differences in the size of the preferred food particles (mainly bacteria). Further investigations are in progress to clarify this point by using inert, artificial food particles of different sizes to determine both the optimal dimensions of the food and the time needed for the ingestion process, as has been studied extensively in species of other heterotrophic flagellate groups e.g. by Boenigk *et al.* (2001a-c, 2002).

Growth rates

The maximal growth rates measured for the three *Caecitellus* strains, i.e. the deep sea strain DQ220712, the surface water strain DQ220713 and the strain DQ230538, were within the range reported for other heterotrophic flagellates (Fenchel 1982b, Sherr *et al.* 1984, Eccleston-Parry and Leadbeater 1994). The ranges of the measured growth rates showed no overlap between the strains, indicating distinct differences. The deep sea strain showed a higher growth rate compared to the surface water strain, even though the growth experiments were conducted under surface water conditions (19 °C, atmospheric pressure). This was not surprising, as it has been repeatedly demonstrated that deep sea heterotrophic flagellates show high growth rates under surface water conditions (Patterson *et al.* 1993, Atkins *et al.* 1998, Arndt *et al.* 2003). The growth rates of the deep sea strain (DQ220712) are closer (though not identical) to those of the DQ230538 strain than to those of the surface water strain from the same region. This finding matches the molecular data which shows that the deep sea and the DQ230538 strain are closely related (both cluster within Clade 1), whereas the surface water strain (DQ220713) clusters within Clade 3. Furthermore, the lower growth rates of the *C. cf.*

Table 4. SSU rDNA signature sequences of *Caecitellus parvulus*, *C. pseudoparvulus* and *C. paraparvulus*.

Species	Sequence signature (5'-3')	Position ¹	Environmental sequences considered
A			
<i>Caecitellus parvulus</i> ²	tacttgatagctcttctactc	118	
	caattctagagctaagacgcgctat	152	
	gtgctcgtagtcggtc	601	AY046666
	ggctggcgcgtgtgct	625	
	ccgccttggcggcc	645	
	cttg	735	AY046666
	gaactgctgcgaaagcg	840	AY046666
	tagaccctggttcagggtgcta	1261	AY046666
	cgcgagtcacatctcgca	1500	AY046666
agcgagctccggctcgtcgagaagttggtt	1596	AY046666	
B			
<i>Caecitellus pseudoparvulus</i> ⁴	atttattagatacaaccacacca	187	
	tggactctacg	446	
	atgcactcccggcca ⁵	601	
	tggcgatgtggagttc ⁵	625	
	cgattgtt ⁵	964	
	cgggctctgtttcagggtgccg ⁵	1261	
	cgaagacccccgctcgacgcgagaactggcta ⁵	1596	
C			
<i>Caecitellus paraparvulus</i> ³	cacttgatagctctctactt	118	AY789784
	gttccggcgctcccgttc	601	AY789784, AM041117
	cggggacacggggacc	625	AJ965041, AJ965066, AJ965067, AY789784
	tacg	735	AJ965041, AJ965066, AJ965067, AM041117, AY789784
	gata	761	AJ965041, AJ965066, AJ965067, AM041117
	cctggcccctgcggc	1596	

¹Position in *Caecitellus pseudoparvulus* DQ230538 used as reference.

²Signature sequences always matching *Caecitellus* AF174367 and AF174368.

³Signature sequences always matching *Caecitellus* AY827847, AY827848, and DQ220713-DQ220716.

⁴Signature sequences always matching *Caecitellus* AY520455, DQ220712, and DQ230538.

⁵Signature sequences also matching *Caecitellus* AY520456.

parvulus strain DQ220713 (from the South Atlantic surface water) coincided with a smaller feeding basket compared to strain DQ220712. This might reflect a strategy of high exploration of resources in the latter, which results in high growth rate under optimal food conditions. However, such conclusions on the link between molecular data, ultrastructure and growth rate need to be taken with caution unless further strains are investigated.

Molecular Data

The high level of genetic divergence within the morphospecies *Caecitellus parvulus* and the high boot-

strap support for the three clades suggest that this species complex represents an assemblage of microscopically similar morphotypes united by morphological traits visible on the level of light-microscopy: one trailing flagellum, one stiffly and slowly moving anterior flagellum, flattened and often triangular in profile (Patterson *et al.* 1993, O'Kelly and Nerad 1998, Lee *et al.* 2000). The present molecular data alone proposes that the morphospecies *C. parvulus* is no longer maintainable as such and that it will need to be divided into three different species. They do not cluster together based on their geographical origins or habitats; strains from the South Atlantic Ocean and the North Atlantic Ocean as well as

strains from the Eastern Pacific Ocean and the North Atlantic Ocean are identical. Besides the molecular data, the only way to reliably distinguish at least two (Clade 1 and Clade 3) of the three lineages is the ultrastructural data including the behavioural observations presented in this study.

Conclusions

The ultrastructural distinction and the large genetic differences between the three clades of the morphospecies *Caecitellus parvulus* as well as the high degree of the genetic similarity within each genotype demonstrate the existence of at least three species within a *Caecitellus* complex.

Recent molecular studies indicate that several cryptic species might exist among protists (e.g. Nanney *et al.* 1998, Darling *et al.* 2004, Scheckenbach *et al.* 2005). At least in some cases, detailed comparisons of morphological and non-morphological features showed that also pseudo-cryptic species exist and that slight morphological differences may separate species (Huber *et al.* 1997, Darling *et al.* 1999, de Vargas *et al.* 1999, Sáez *et al.* 2003, Sáez and Lozano 2005). Therefore the results of the present study led to descriptions of two new *Caecitellus* species. One called *Caecitellus paraparvulus* includes the strains of Clade 1 of this study; the other new species, named *Caecitellus pseudoparvulus*, includes both strains of Clade 3 (Fig. 35). O'Kelly and Nerad (1998) presented only light microscopical photographs of the now newly designated strain *Caecitellus pseudoparvulus* DQ230538, isolated from the Sargasso Sea. For the ultrastructural description of *Caecitellus parvulus* they used the strain ATCC50712, which was isolated from the North Pacific Ocean. Unfortunately this strain is no longer available from the American Type Culture Collection, were it was deposited (O'Kelly and Nerad 1998). Therefore it does not seem to be possible to investigate the genotype of this strain at present. Clade 2 includes two strains of *C. parvulus* which were sequenced and described by Atkins *et al.* (2000) using light microscopy.

As pointed out by de Vargas *et al.* (1999) for planktonic foraminifers, our results (including the results of Scheckenbach *et al.* 2005) indicate that the worldwide species diversity of *Caecitellus parvulus* - as a case study of heterotrophic nanoflagellates - might be greatly underestimated if a morphospecies concept is exclusively applied. Different strains of the three species of the genus *Caecitellus* were found in different loca-

tions or habitats. Consequently it seems there is no evidence for endemism of the *Caecitellus* species, but special micro-environment and behavioural conditions might exist.

Finally, our results show the potential of combined DNA, ultrastructural and behavioural analyses for detection of species complexes within morphospecies of heterotrophic flagellates.

Taxonomic Diagnosis (Table 3)

Genus *Caecitellus* (Patterson *et al.* 1993)

Distinguishable at the level of light microscopy among gliding flagellates by a conspicuous ventral mouth, the orientation of the two flagella and the beat pattern of the anterior flagellum (Al-Qassab *et al.* 2002). Cell sizes from 2-10 µm have been reported. The small heterotrophic nanoflagellates have somewhat rounded or triangular profiles and feed on bacteria. The anterior flagellum inserts apically, is about 1-2.5 times the cell length and beats anteriorly and stiffly. The measurements for the length of the posterior trailing flagellum range from 2 to 4.5 times the cell length (e.g. Griessmann 1913, Larsen and Patterson 1990, Patterson *et al.* 1993, O'Kelly and Nerad 1998, Tong *et al.* 1998, Lee and Patterson 2000, Al-Qassab *et al.* 2002, Lee *et al.* 2003, present study).

Caecitellus parvulus (Basionym: *Bodo parvulus*, Griessmann 1913) Patterson *et al.* (1993). For detailed ultrastructural description see O'Kelly and Nerad (1998). Sequence signature see Table 4 A.

Caecitellus pseudoparvulus n. sp.

The kinetid of *Caecitellus pseudoparvulus* is basically similar to the kinetid of *C. parvulus* as described by O'Kelly and Nerad (1998). Different is the maximal number of microtubules of the large loop of R3. 35 microtubules were counted in the cytostome for *C. pseudoparvulus*. An additional microtubule x' is located in the area of the turning point of the large loop directly underneath microtubule x, first described in this study for *C. pseudoparvulus* and *C. paraparvulus*. Within the *Caecitellus*-complex only *C. pseudoparvulus* shows a relatively thick electron-dense glycocalyx. *C. pseudoparvulus* has on the average a longer posterior flagellum than *Caecitellus paraparvulus*. Sequence signature see Table 4 B.

Caecitellus paraparvulus n. sp.

The first-described *Caecitellus* species, *C. paraparvulus*, has basically the same ultrastructure as described by O'Kelly and Nerad (1998) for

C. parvulus. Different is the maximal number of microtubules of the large loop of R3. With approximately 29 microtubules, *C. paraparvulus* has five microtubules more than *C. parvulus* and six microtubules fewer than *C. pseudoparvulus* in its feeding basket. As described for *C. pseudoparvulus*, there is an x'-microtubule underneath the x-microtubule. The glycocalyx of *C. paraparvulus* is thin or hardly visible without special staining procedures. Compared to *C. pseudoparvulus*, this species usually has a shorter posterior flagellum. Sequence signature see Table 4 C.

Acknowledgements. This study was funded by the German Research Foundation (DFG; Ar 288/5-1 and HA 818/18-1). We would like to thank Prof. Diethard Tautz (University of Cologne, Institute of Genetics, Cologne, Germany) for helpful comments and discussions. We also thank the scientific illustrator Peter Adam (Free University of Berlin, Institute of Biology / Zoology, Berlin, Germany) for preparing Figs 36 and 37.

REFERENCES

- Al-Qassab S., Lee W. J., Murray S., Simoson A. G. B., Patterson D. J. (2002) Flagellates from stromatolites and surrounding sediments in Shark Bay, Western Australia. *Acta Protozool.* **41**: 91-144
- Arndt H., Dietrich D., Auer B., Cleven E.-J., Gräfenhan T., Weitere M., Mylnikov A. P. (2000) Functional diversity of heterotrophic flagellates in aquatic ecosystems. In: The Flagellates, (Eds. B. S. C. Leadbeater., J. C. Green). Systematics Association Special Publications. Taylor & Francis, London, 240-268
- Arndt H., Hausmann K., Wolf M. (2003) Deep sea heterotrophic nanoflagellates of the Eastern Mediterranean Sea: qualitative and quantitative aspects of their pelagic and benthic occurrence. *Mar. Ecol. Prog. Ser.* **256**: 45-56
- Atkins M. S., Anderson O. R., Wirsén C. O. (1998) Effects of hydrostatic pressure on the growth rates and encystment of flagellated protozoa isolated from a deep-sea hydrothermal vent and a deep shelf region. *Mar. Ecol. Prog. Ser.* **171**: 85-95
- Atkins M. S., Teske A. P., Anderson O. R. (2000) A survey of flagellate diversity at four deep-sea hydrothermal vents in the Eastern Pacific Ocean using structural and molecular approaches. *J. Euk. Microbiol.* **47**: 400-411
- Azam F., Fenchel T., Field J.G., Gray J. S., Meyer-Reil L. A., Thingstad F. (1983) The ecological role of water-column microbes in the sea. *Mar. Ecol. Prog. Ser.* **10**: 257-263
- Berninger U.-G., Finlay B. J., Kuuppo-Leinikki P. (1991) Protozoan control of bacterial abundances in freshwater. *Limnol. Oceanogr.* **36**: 139-147
- Boenigk J., Arndt H. (2002) Bacterivory by heterotrophic flagellates: community structure and feeding strategies. *Antonie van Leeuwenhoek* **81**: 465-480.
- Boenigk J., Arndt H., Cleven E. J. (2001a) The problematic nature of fluorescently labeled bacteria (FLB) in *Spumella* feeding experiments - an explanation by using video microscopy. *Arch. Hydrobiol.* **152**: 329-338
- Boenigk J., Matz C., Jürgens K., Arndt H. (2001b) The influence of preculture conditions and food quality on the ingestion and digestion process of three species of heterotrophic nanoflagellates. *Microbiol. Ecol.* **42**: 168-176
- Boenigk J., Matz C., Jürgens K., Arndt H. (2001c) Confusing selective feeding with differential digestion in bacterivorous nanoflagellates. *J. Euk. Microbiol.* **48**: 425-432
- Boenigk J., Matz C., Jürgens K., Arndt H. (2002) Food concentration dependent regulation of food selectivity of interception feeding bacterivorous nanoflagellates. *Aquatic Microbiol. Ecol.* **27**: 195-202
- Caron D. A. (1991) Heterotrophic flagellates associated with sedimenting detritus. In: The Biology of Free-living Heterotrophic Flagellates, (Eds. D. J. Patterson, J. Larsen). Clarendon Press, Oxford, 77-92
- Clark G. C. (1992) Riboprinting: a molecular approach to the identification and taxonomy of protozoa. In: Protocols in Protozoology, (Eds. J. J. Lee, A. T. Soldo). Allen, Lawrence, Kansas, D4.1-D4.4
- Darling K. F., Wade C. M., Kroon D., Leigh Brown A. J., Bijam J., (1999) The diversity and distribution of modern planktonic foraminiferal small subunit ribosomal RNA genotypes and their potential as tracers of present and past ocean circulations. *Paleoceanography* **14**: 3-12
- Darling K. F., Kucera M., Pudsey C. J., Wade C.M. (2004) Molecular evidence links cryptic diversification in polar planktonic protists to quaternary climate dynamics. *Proc. Natl. Acad. Sci. USA* **101**: 7657-7662
- de Vargas C., Norris R., Zaninetti L., Pawlowski J. (1999) Molecular evidence of cryptic speciation in planktonic foraminifers and their relation to oceanic provinces. *Proc. Natl. Acad. Sci. USA* **96**: 2864-2868
- Eccleston-Parry J. D., Leadbeater B. S. C. (1994) The effect of long-term low bacterial density on the growth kinetics of three marine heterotrophic microflagellates. *J. Exp. Mar. Biol. Ecol.* **117**: 219-233
- Ekeboom J., Patterson D. J., Vørs N. (1995/1996) Heterotrophic flagellates from coral reef sediments (Great Barrier Reef, Australia). *Arch. Protistenkd.* **146**: 251-272
- Felsenstein J. (1981) Evolutionary trees from gene frequencies and quantitative characters: finding maximum likelihood estimates. *Evolution* **35**: 1229-1242
- Felsenstein J. (1985) Confidence limits on phylogenies: an approach using the bootstrap. *Evolution* **39**: 783-791
- Felsenstein J. (2004) PHYLIP (Phylogeny Inference Package) version 3.63. Distributed by the author. Department of Genome Sciences, University of Washington, Seattle
- Fenchel T. (1982a) Ecology of heterotrophic microflagellates. I. Some important forms and their functional morphology. *Mar. Ecol. Prog. Ser.* **8**: 211-223
- Fenchel T. (1982b) Ecology of heterotrophic flagellates. II. Bioenergetics and growth. *Mar. Ecol. Prog. Ser.* **8**: 225-231
- Finlay B. J. (2002) Global dispersal of free-living microbial eukaryote species. *Science* **296**: 1061-1063
- Foissner W. (1999) Protist diversity: estimates of the near-imponderable. *Protist* **150**: 363-368
- Gasol J. M., Vaqué D. (1993) Lack of coupling between heterotrophic nanoflagellates and bacteria: a general phenomenon across aquatic systems? *Limnol. Oceanogr.* **38**: 657-665
- Griessmann K. (1913) Über marine Flagellaten. *Arch. Protistenkd.* **32**: 1-78
- Hausmann K., Weitere M., Wolf M., Arndt H. (2002) *Meteora sporadica* gen. et sp. nov. (Protista incertae sedis) - an extraordinary free-living protist from the Mediterranean deep sea. *Europ. J. Protistol.* **38**: 171-177
- Huber B., Bijama J., Darling K. (1997) Cryptic speciation in the living planktonic foraminifer *Globigerinella siphonifera* (d'Orbigny). *Paleobiology* **23**: 33-62
- Karpov S. A., Sogin M. L., Silberman J. D. (2001) Rootlet homology, taxonomy, and phylogeny of bicosoecids based on 18S rRNA gene sequences. *Protistology* **2**: 34-47
- Kjørboe T., Grossart H.-P., Ploug H., Tang K., Auer B. (2004) Particle-associated flagellates: swimming patterns, colonizing rates, and grazing on attached bacteria. *Aquat. Microb. Ecol.* **35**: 141-152
- Kumar S., Tamura K., Nei M. (2004) MEGA3: Integrated software for Molecular Evolutionary Genetics Analysis and sequence alignment. Briefings in Bioinformatics 5:2

- Larsen J., Patterson D. J. (1990) Some flagellates (Protista) from tropical marine sediments. *J. Nat. Hist.* **24**: 801-937
- Lee J. J., Leedale G. F., Bradbury P. (Eds.) (2000) An Illustrated Guide to the Protozoa, 2nd ed. Allen Press Inc., Lawrence, KS, USA
- Lee W. J., Patterson D. J. (1998) Diversity and geographic distribution of free-living heterotrophic flagellates - analysis by PRIMER. *Protist* **149**: 229-244
- Lee W. J., Patterson D. J. (2000) Heterotrophic flagellates (Protista) from marine sediments of Botany Bay, Australia. *J. Nat. Hist.* **34**: 483-562
- Lee W. J., Brandt S. M., Vørs N., Patterson D. J. (2003) Darwin's heterotrophic flagellates. *Ophelia* **57**: 63-98
- Lockhart F. J., Steel M. A., Hendy M. D., Penny D. (1994) Recovering evolutionary trees under a more realistic model of sequence evolution. *Mol. Biol. Evol.* **11**: 605-612
- Mayden R. L. (1997) A hierarchy of species concepts: the denouement in the saga of species problem. In: Species: the Units of Biodiversity, (Eds. M. F. Claridge, H. A. Dawah., M. R. Wilson). London, Chapman and Hall, 381-424
- Moestrup Ø. (1995) Current status of chrysophyte "splinter groups": synurophytes, pedinellids, silicoflagellates. In: Chrysophyte Algae: Ecology, Phylogeny, Development, (Eds. C. Sangren, J. P. Smol, J. Kristiansen). Cambridge University Press, Cambridge, UK, 75-91
- Nanney D. L., Park C., Preparata R., Simon E. M. (1998) Comparison of sequence differences in a variable 23S rRNA domain among sets of cryptic species of ciliated protozoa. *J. Euk. Microbiol.* **45**: 91-100
- O'Kelly C. J., Nerad T. A. (1998) Kinetid architecture and bicosoecid affinities of the marine heterotrophic nanoflagellate *Caecitellus parvulus* (Griessmann 1913) Patterson *et al.* (1993). *Europ. J. Protistol.* **34**: 369-375
- Page F. C., Blakey S. M. (1979) Cell surface structure as a taxonomic character in the Thecamoebidae (Protozoa: Gymnamoebia). *Zoo. J. Linn. Soc.* **66**: 113-135
- Parducz B. (1967) Ciliary movement and coordination in ciliates. *Int. Rev. Cytol.* **21**: 91-128
- Patterson D. J., Simpson A. G. B. (1996) Heterotrophic flagellates from coastal marine and hypersaline sediments in Western Australia. *Europ. J. Protistol.* **32**: 423-448
- Patterson D. J., Lee W. J. (2000) Geographic distribution and diversity of free-living heterotrophic flagellates. In: The Flagellates, (Eds. B. S. C. Leadbeater, J. C. Green). Systematics Association Special Publications. Taylor & Francis, London, 269-287
- Patterson D. J., Nygaard K., Steinberg G., Turley C. M. (1993) Heterotrophic flagellates and other protists associated with oceanic detritus throughout the water column in the North Atlantic. *J. Mar. Biol. Assoc. UK* **73**: 67-95
- Porter K. G., Feig Y. S. (1980) The use of DAPI for identifying and counting aquatic microflora. *Limnol. Oceanogr.* **25**: 943-948
- Preisig H. R., Vørs N., Hällfors G. (1991) Diversity of heterotrophic heterokont flagellates. In: The Biology of Free-living Heterotrophic Flagellates, (Eds. D. J. Patterson, J. Larsen). Clarendon Press, Oxford, 361-400
- Rzhetsky A., Nei M. (1992) A simple method for estimating and testing minimum-evolution trees. *Mol. Biol. Evol.* **9**: 945-967
- Sáez A. G., Lozano E. (2005) Body doubles. Cryptic species: as we discover more examples of species that are morphologically indistinguishable, we need to ask why and how they exist. *Nature* **433**: 111
- Sáez A. G., Probert I., Geisen M., Quinn P., Young J. R., Medlin L. K. (2003) Pseudo-cryptic speciation in coccolithophores. *Proc. Natl. Acad. Sci. USA* **100**: 7163-7168
- Scheckenbach F., Wylezich C., Weitere M., Hausmann K., Arndt H. (2005) Molecular identity of strains of heterotrophic flagellates isolated from surface waters and deep sea sediments of the South Atlantic based on SSU rDNA. *Aquat. Microb. Ecol.* **38**: 239-247
- Schlegel M., Meisterfeld R. (2003) The species problem in protozoa revisited. *Europ. J. Protistol.* **39**: 349-355
- Sherr B. F., Sherr E. B., Newell S. Y. (1984) Abundance and productivity of heterotrophic nanoplankton in Georgia coastal waters. *J. Plankt. Res.* **6**: 195-202
- Sims G. P., Aitken R., Rogerson A. (2002) Identification and phylogenetic analysis of morphologically similar naked amoebae using small subunit ribosomal RNA. *J. Euk. Microbiol.* **49**: 478-484
- Steel M. A. (1994) Recovering a tree from the leaf colourations it generates under a Markov model. *Appl. Math. Lett.* **7**: 19-24
- Swofford D. L., Olsen G. J. (1990) Phylogeny reconstruction. In: Molecular Systematics, (Eds. D. M. Hillis, C. Moritz). Sinauer Associates, Sunderland, 411-501
- Thompson J. D., Higgins D. G., Gibson T. J. (1994) CLUSTAL W: improving the sensitivity of progressive multiple alignment through sequence weighting, positions-specific gap penalties and weight matrix choice. *Nucleic Acids Res.* **22**: 4673-4680
- Tong S. M. (1997a) Heterotrophic flagellates from the water column in Shark Bay, Western Australia. *Mar. Biol.* **128**: 517-536
- Tong S. M. (1997b) Heterotrophic flagellates and other protists from Southampton water. *Ophelia* **47**: 71-131
- Tong S. M., Nygaard K., Bernard C., Vørs N., Patterson D. J. (1998) Heterotrophic flagellates from the water column in Port Jackson, Sydney, Australia. *Europ. J. Protistol.* **34**: 162-194
- Turley C. (2002) The importance of "marine snow". *Microbiol. Today* **29**: 177-179

Received on 25th April, 2006; revised version on 10th July, 2006; accepted on 13th September, 2006